Improved algorithm for analytical solution of the heat conduction problem in doubly periodic 2D composite materials

D. Kapanadze[1], G. Mishuris[2] *, E. Pesetskaya[1†]

[1] A. Razmadze Mathematical Institute, Tbilisi State University, Georgia
(daka@rmi.ge,kate.pesetskaya@gmail.com)
[2] Institute of Mathematics and Physics, Aberystwyth University, UK
(ggm@aber.ac.uk).

Abstract

We consider a boundary value problem in unbounded 2D doubly periodic composite with circular inclusions having arbitrary constant conductivities. By introducing complex potentials, the boundary value problem for the Laplace equation is transformed to a special R-linear BVP for doubly periodic analytic functions. This problem is solved with use of the method of functional equations. The R-linear BVP is transformed to a system of functional equations. A new improved algorithm for solution of the system is proposed. It allows one not only to compute the average property but to reconstruct the solution components (temperature and flux) at an arbitrary point of the composite. Several computational examples are discussed in details demonstrating high efficiency of the method. Indirect estimate of the algorithm accuracy has been also provided.

Keywords: steady-state conductivity problem, boundary value problems, periodic structure, 2D unbounded composite material, elliptic functions, flux distribution, temperature distribution, effective conductivity

AMS: 30E25, 35B27, 74Q05, 33E05

1 Introduction

Heterogeneous media model problems serve the purposes of material science studies for the analysis of the various fields and prediction of their properties [4, 15, 17, 26]. Different approaches for study linear inhomogeneous material are presented in well-known monographs [1, 7, 13, 16, 18, 22]. One of the

*supported by the FP7 PEOPLE IAPP Project PARM-2 under number 284544.
†supported by Shota Rustaveli National Science Foundation FR/6/5-101/12.

approaches dealing with composite materials is the so-called homogenization method (see [3, 10]). Mathematical aspects of the higher order homogenization have been developed in [5]. The limiting case for large (close to the maximal value) rectangular cross-section cylindrical cavities by means of an asymptotic procedure were studied in [3] where explicit analytical expressions for effective parameters have been also found. Non-local phenomena resulting from a high contrast (or anisotropy) of composite structures were studied in [1, 6]. In two- and three-dimensional cases the Rayleigh multipole expansions method and its generalizations is effectively used (see, e.g. [22]). Various analytical approaches have been discussed in [21, 23].

Essential progress has been already achieved in the area of numerical analysis of composite material properties. Such approach is naturally restricted to a finite cell (or a few cell - representative element) size in order to reduce the computation cost. A vast literature related to this approach can be found in [28]. The major advantage of analytical approach is a possibility to describe and analyze the material properties by means of explicit analytical formulas. This allow one to reveal an influence of the materials characteristics (like size, shape, location of components, their material properties) on the overall properties of the composite (homogeneous approach) [2, 4, 8, 11, 14, 20, 24]. Recently, the relationship between the effective properties in the problem of the heat conduction and elasticity have been revealed and effectively exploited [12, 25].

In this paper, we reveal another advantage of the analytical approach showing that it is capable to efficiently reconstruct the global and local distributions of the physical fields. We consider well-known linear heat conduction problem in 2D unbounded doubly periodic composite with material properties independent of the temperature field. The components (inclusions) are supposed to be disjoint disks formed a doubly periodic structure. We consider the steady process governed here by the Laplace equation. We will mostly follow by pioneering work [4], but a few important improvements will be introduced. First, we slightly change the problem formulation introducing more natural conditions at infinity prescribing only average flux, at an arbitrary direction, in contrast to the problem investigated in [4], where a special temperature distribution assumed in the direction of the coordinate system. In the linear formulation, our approach is in fact equivalent to periodic conditions for flux on the boundary of the minimal representative cell.

Although, we treat the problem using the methods developed in [4], reduc-

ing the corresponding BVP to a system of functional equations with respect to doubly periodic analytical functions, we substantially change the algorithm for the numerical calculations. The algorithm in [4] is mostly oriented to find the effective conductivity. In this case, it is sufficient to know values of the heat flux in the centers of inclusions only. However, it turns out that it may not guarantee the best accuracy when defining values of the flux outside the inclusion or reconstructing the temperature distribution. Modified algorithm presented in this work allows one to increase an accuracy of the numerical computations an any point in the distance from the centers of inclusions and to find the temperature field (with accuracy to an arbitrary constant). The proposed modification allows us to find the flux distribution in an explicit form containing all parameters of the considered model such as conductivities of the matrix and inclusions, radii and centers of inclusions, an intensity and an angle of the flux. As the previous algorithm, it also relays on the values of special Eisenstein functions ([27]).

The paper is organized as follows. In Section 2 we describe the geometry of the considered composites and formulate the mathematical problem basing on proper physical assumptions. In Section 3 we briefly overview the auxiliary problem stated in [4], show a connection with the original problem.

In Section 4 we describe a new algorithm in details and show that both components of the solution, the flux and the temperature, can be computed in the unique scheme. Finally, numerical calculations are performed and discussed in Section 5 to demonstrate algorithm accuracy, robustness and effectiveness.

2 Statement of the problem

We consider a lattice L which is defined by the two fundamental translation vectors "1" and "$\imath$" (where $\imath^2 = -1$) in the complex plane $\mathbb{C} \cong \mathbb{R}^2$ (with the standard notation $z = x + \imath y$).

Here, the representative cell (see Fig. 1) will be the square

$$Q_{(0,0)} := \left\{ z = t_1 + \imath t_2 \in \mathbb{C} : -\frac{1}{2} < t_p < \frac{1}{2},\, p = 1, 2 \right\}. \tag{1}$$

Let $\mathcal{E} := \bigcup\limits_{m_1, m_2} \{m_1 + \imath m_2\}$ be the set of the lattice points, where $m_1, m_2 \in \mathbb{Z}$.

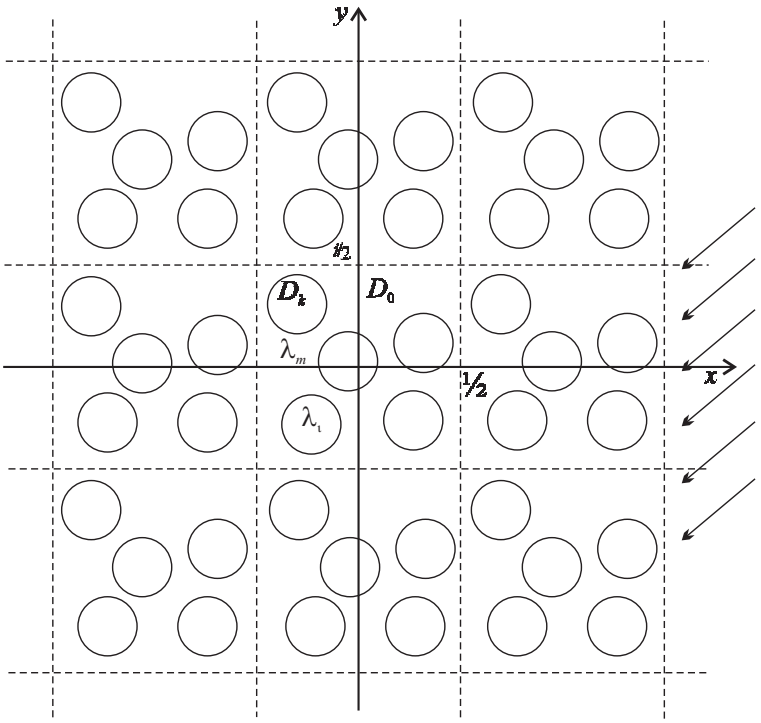

Figure 1: The representative cell $Q_{(0,0)}$ within doubly periodic composite.

The cells corresponding to the points of the lattice $\mathcal{E}$ will be denoted by

$$Q_{(m_1,m_2)} = Q_{(0,0)} + m_1 + \imath m_2 := \left\{ z \in \mathbb{C} : z - m_1 - \imath m_2 \in Q_{(0,0)} \right\}. \qquad (2)$$

It is considered the situation when mutually disjoint disks (inclusions) $D_k := \{z \in \mathbb{C} : |z - a_k| < R\}$ with a radius R and boundaries $\partial D_k := \{z \in \mathbb{C} : |z - a_k| = R\}\,(k = 1, 2, \ldots, N)$ are located inside the cell $Q_{(0,0)}$ and periodically repeated in all cells $Q_{(m_1,m_2)}$. Let us denote by

$$D_0 := Q_{(0,0)} \setminus \left(\bigcup_{k=1}^{N} D_k \cup \partial D_k \right) \qquad (3)$$

the connected domain obtained by removing of the inclusions from the cell $Q_{(0,0)}$ (cf. Fig. 1).

Let us consider the problem of determination of the heat flux function of

a doubly periodic composite material with matrix

$$D_{matrix} = \bigcup_{m_1,m_2} ((D_0 \cup \partial Q_{(0,0)}) + m_1 + \imath m_2) \tag{4}$$

and inclusions

$$D_{inc} = \bigcup_{m_1,m_2} \bigcup_{k=1}^{N} (D_k + m_1 + \imath m_2) \tag{5}$$

occupied by materials of conductivities $\lambda_m > 0$ and $\lambda_i > 0$, respectively. For this purpose, we consider a problem of the determination of the potential of the corresponding fields, i.e., a temperature function $T = T(x, y)$ satisfying the Laplace equation in each component of the composite material

$$\Delta T(z) = 0, \qquad z \in D_{matrix} \cup D_{inc}, \tag{6}$$

which have to satisfy the following boundary conditions on all ∂D_k, $k = 1, 2, \ldots, N$:

$$T(t) = T_k(t), \tag{7}$$

$$\lambda_m \frac{\partial T}{\partial n}(t) = \lambda_i \frac{\partial T_k}{\partial n}(t), \qquad t \in \bigcup_{m_1,m_2} \partial D_k. \tag{8}$$

Here, the vector $n = (n_1, n_2)$ is the outward unit normal vector to ∂D_k, $\frac{\partial}{\partial n} = n_1 \frac{\partial}{\partial x} + n_2 \frac{\partial}{\partial y}$ is the outward normal derivative, and

$$T(t) := \lim_{z \to t, z \in D_0} T(z), \qquad T_k(t) := \lim_{z \to t, z \in D_k} T(z). \tag{9}$$

The conditions (7)–(8) form the so-called *ideal (perfect) contact conditions*.

The thermal loading for the composite is described weakly by the flux given at infinity or more accurately by its intensity A. We assume that the flux is directed θ which does not coincide, in general, with the orientation of the periodic cell (see, Fig. 1). According to the conservation law and the ideal contact condition between the different materials, the flux is continuous in the entire structure. Moreover, as a result of such formulation, the temperature, which is also continuous as the results of the ideal transmission conditions along the interface between the matrix and inclusions, possesses non-zero jumps across any cell.

In addition, we assume that the heat flux is periodic on y. Thus,

$$\lambda_m T_y\Big(x, \frac{1}{2}\Big) = \lambda_m T_y\Big(x, -\frac{1}{2}\Big) = -A \sin\theta + q_1(x), \tag{10}$$

where A is the intensity of an external flux. The heat flux is periodic on x, consequently,

$$\lambda_m T_x\Big(-\frac{1}{2}, y\Big) = \lambda_m T_x\Big(\frac{1}{2}, y\Big) = -A\cos\theta + q_2(y). \tag{11}$$

To complement to the average flux conditions at infinity, the latter immediately proves that the equalities

$$\int\limits_{-1/2}^{1/2} q_j(\xi)d\xi = 0 \tag{12}$$

are valid for the unknown functions q_j, $(j = 1, 2)$. As a result of (10) and (11), the heat flux has a zero mean value along the cell

$$\int\limits_{\partial Q_{(m_1,m_2)}} \frac{\partial T(s)}{\partial n} ds = 0. \tag{13}$$

From the physics point of view, condition (13) is the consequence of the fact that no source (sink) exists in the cells. Moreover, since there is no source (sink) inside the composite, i.e., neither in the matrix of the composite, nor in any inclusion (the total heat flux through any closed simply connected curve is equal to zero), we have

$$\int\limits_{\partial D_k + m_1 + \imath m_2} \frac{\partial T}{\partial n} ds = 0. \tag{14}$$

We will introduce complex potentials $\varphi(z)$ and $\varphi_k(z)$ which are analytic in D_0 and D_k, and continuously differentiable in the closures of D_0 and D_k, respectively, by using the following relations

$$T(z) = \begin{cases} \operatorname{Re}\left(\varphi(z) + Bz\right),\ z \in D_{matrix}, \\ \\ \frac{2\lambda_m}{\lambda_m + \lambda_i} \operatorname{Re}\varphi_k(z),\ z \in D_{inc}, \end{cases} \tag{15}$$

where B is an unknown constant belong to $\mathbb{C}$. Besides, we assume the the real part of φ is doubly periodic in D_0, i.e.

$$\operatorname{Re}\varphi(z+1) - \operatorname{Re}\varphi(z) = 0, \qquad \operatorname{Re}\varphi(z+\imath) - \operatorname{Re}\varphi(z) = 0.$$

Note that in general the imaginary part of φ is not doubly periodic in D_0.

Let us show that φ is single-valued function in D_{matrix}. We take a harmonic function v in D_{matrix} which is the harmonic conjugate to T. For this pair of functions the Cauchy-Riemann equations $\frac{\partial T}{\partial x} = \frac{\partial v}{\partial y}$, $\frac{\partial T}{\partial y} = -\frac{\partial v}{\partial x}$ (or the so called normal-tangent Cauchy-Riemann equations $\frac{\partial T}{\partial n} = \frac{\partial v}{\partial s}$, $\frac{\partial T}{\partial s} = -\frac{\partial v}{\partial n}$) have to be valid. The functions v has the following form:

$$v(z) = \begin{cases} \operatorname{Im}(\varphi(z) + Bz), \ z \in D_{matrix}, \\ \\ \frac{2\lambda_m}{\lambda_m + \lambda_i} \operatorname{Im} \varphi_k(z), \ z \in D_{inc}, \end{cases} \tag{16}$$

with the same unknown constant B.

As it follows from (13) – (14) we can write

$$\int\limits_{\partial Q_{(m_1,m_2)}} \frac{\partial v}{\partial s} ds = 0, \qquad \int\limits_{\partial D_k + m_1 + \imath m_2} \frac{\partial v}{\partial s} ds = 0. \tag{17}$$

These relations yield that the harmonic function v is single-valued in the domain D_{matrix}. Therefore, the complex potential $\varphi(z)$ is single-valued in D_{matrix}.

To determine the flux $\nabla T(x, y)$, we need to obtain derivatives of the complex potentials:

$$\begin{aligned} \psi(z) &:= \tfrac{\partial \varphi}{\partial z} = \tfrac{\partial T}{\partial x} - \imath \tfrac{\partial T}{\partial y} - B, && z \in D_0, \\ \psi_k(z) &:= \tfrac{\partial \varphi_k}{\partial z} = \tfrac{\lambda_m + \lambda_i}{2\lambda_m} \left(\tfrac{\partial T_k}{\partial x} - \imath \tfrac{\partial T_k}{\partial y} \right), && z \in D_k. \end{aligned} \tag{18}$$

Let us rewrite conditions (7)–(8) in terms of the complex potentials $\varphi(z)$ and $\varphi_k(z)$. Let s be the natural parameter of the curve ∂D_k and

$$\frac{\partial}{\partial s} = -n_2 \frac{\partial}{\partial x} + n_1 \frac{\partial}{\partial y} \tag{19}$$

be the tangent derivative along ∂D_k. Applying the Cauchy-Riemann equations, the equality (8) can be written as

$$\lambda_m \frac{\partial v}{\partial s}(t) = \lambda_i \frac{\partial v_k}{\partial s}(t), \qquad |t - a_k| = R. \tag{20}$$

Integrating the last equality on s, we arrive at the relation

$$\lambda_m v(t) = \lambda_i v_k(t) + c, \tag{21}$$

where c is an arbitrary constant. We put $c = 0$ since the imaginary part of the function φ is determined up to an additive constant which does not impact on the form of T. Using (16), we have

$$\mathrm{Im}\,\varphi(t) = -\mathrm{Im}\,(Bt) + \frac{2\lambda_i}{\lambda_m + \lambda_i}\mathrm{Im}\,\varphi_k(t), \qquad |t - a_k| = R. \tag{22}$$

Using (15), we are able to write the equality (7) in the following form:

$$\mathrm{Re}\,\varphi(t) = -\mathrm{Re}\,(Bt) + \frac{2\lambda_m}{\lambda_m + \lambda_i}\mathrm{Re}\,\varphi_k. \tag{23}$$

Adding the relation (23) and (22) multiplied by $\imath$, and using $\mathrm{Re}\,\varphi_k = \frac{\varphi_k + \overline{\varphi_k}}{2}$, $\mathrm{Im}\,\varphi_k = \frac{\varphi_k - \overline{\varphi_k}}{2\imath}$, $t - a_k = \frac{r_k^2}{\overline{t - a_k}}$, we have

$$\varphi(t) = \varphi_k(t) - \rho\overline{\varphi_k(t)} - Bt, \qquad |t - a_k| = R, \tag{24}$$

where $\rho = \frac{\lambda_i - \lambda_m}{\lambda_i + \lambda_m}$.

Let us now differentiate (24). First, note that

$$[\overline{\varphi(t)}]' = -\left(\frac{r_k}{t - a_k}\right)^2 \overline{\varphi'(t)}, \qquad |t - a_k| = R. \tag{25}$$

This can be easily shown by representing the function φ in the form $\varphi(z) = \sum_{l=0}^{\infty} \alpha_k (z - a_k)^l$, $|z - a_k| \le R$, and by using the relation $t = \frac{R^2}{\overline{t - a_k}} + a_k$ on the boundary $|t - a_k| = R$. Thus, after differentiating (24) and using (18), we arrive at the following $\mathbb{R}$-*linear conjugation problem* ([21]) on each contour $|t - a_k| = R$,

$$\psi(t) = \psi_k(t) + \rho\left(\frac{R}{t - a_k}\right)^2 \overline{\psi_k(t)} - B, \tag{26}$$

with $k = 1, 2, \ldots, N$.

Remark 2.1 *Thus, the boundary value problem (6)-(8), (10)-(11) for harmonic functions is reduced to $\mathbb{R}$-linear conjugation problem (26) for analytical doubly periodic functions $\psi, \psi_1, \ldots, \psi_N$.*

We will seek a solution $\psi(z), \psi_k(z)$ of the problem (26) as a sum $\psi(z) = \psi^{(1)}(z) + \psi^{(2)}(z)$, $\psi_k(z) = \psi_k^{(1)}(z) + \psi_k^{(2)}(z)$ of solutions of the following two BVPs:

$$\psi^{(1)}(t) = \psi_k^{(1)}(t) + \rho\left(\frac{R}{t - a_k}\right)^2 \overline{\psi_k^{(1)}(t)} - B_1, \tag{27}$$

$$\psi^{(2)}(t) = \psi_k^{(2)}(t) + \rho\left(\frac{R}{t-a_k}\right)^2 \overline{\psi_k^{(2)}(t)} - \imath B_2, \tag{28}$$

where $\psi_k^{(1)}$ and $\psi_k^{(2)}$ are analytical doubly periodic functions, $B = B_1 + \imath B_2$.

3 Formulation of an auxiliary problem

In this section we briefly overview the auxiliary problem discussed in [4] and represent necessary results in convenient for us form. Let $\widetilde{T}$ be a solution of the boundary value problem (6)-(8) with a constant jump corresponding to the external field applied in the x-direction

$$\widetilde{T}(z+1) = \widetilde{T}(z) + 1, \quad \widetilde{T}(z+\imath) = \widetilde{T}(z). \tag{29}$$

The complex potentials $\widetilde{\varphi}^{(1)}(z)$ and $\widetilde{\varphi}_k^{(1)}(z)$ are introduced as follows

$$\widetilde{T}(z) = \begin{cases} \operatorname{Re}\left(\widetilde{\varphi}^{(1)}(z) + z\right), \ z \in D_{matrix}, \\ \\ \frac{2\lambda_m}{\lambda_m+\lambda_i} \operatorname{Re} \widetilde{\varphi}_k^{(1)}(z), \ z \in D_{inc}. \end{cases} \tag{30}$$

Note that $\widetilde{\varphi}^{(1)}(z)$ and $\widetilde{\varphi}_k^{(1)}(z)$ are analytic in D_0 and D_k, and continuously differentiable in the closures of D_0 and D_k, respectively. Besides, the real part of $\widetilde{\varphi}^{(1)}$ is doubly periodic in D_0, i.e.

$$\operatorname{Re}\widetilde{\varphi}^{(1)}(z+1) - \operatorname{Re}\widetilde{\varphi}^{(1)}(z) = 0, \qquad \operatorname{Re}\widetilde{\varphi}^{(1)}(z+\imath) - \operatorname{Re}\widetilde{\varphi}^{(1)}(z) = 0. \tag{31}$$

In general, the imaginary part of $\widetilde{\varphi}^{(1)}$ is not doubly periodic in D_0. It turns out that they satisfy the following $\mathbb{R}$-linear conjugation boundary value problem obtained in [4]:

$$\widetilde{\varphi}^{(1)}(t) = \widetilde{\varphi}_k^{(1)}(t) - \rho\overline{\widetilde{\varphi}_k^{(1)}(t)} - t, \qquad |t - a_k| = R. \tag{32}$$

Differentiating the last equality, we obtain that the boundary value problem (6)-(8), (29) is reduced to the $\mathbb{R}$-linear conjugation boundary value problem for analytical doubly periodic functions $\widetilde{\psi}^{(1)}, \widetilde{\psi}_1^{(1)}, \ldots, \widetilde{\psi}_N^{(1)}$ (cf. [4]):

$$\widetilde{\psi}^{(1)}(t) = \widetilde{\psi}_k^{(1)}(t) + \rho\left(\frac{R}{t-a_k}\right)^2 \overline{\widetilde{\psi}_k^{(1)}(t)} - 1 \tag{33}$$

with

$$\frac{\partial \widetilde{T}}{\partial x} - \imath \frac{\partial \widetilde{T}}{\partial y} = \begin{cases} \widetilde{\psi}^{(1)}(z) + 1, \ z \in D_{matrix}, \\ \\ \frac{2\lambda_m}{\lambda_m + \lambda_i} \widetilde{\psi}_k^{(1)}(z), \ z \in D_{inc}, \end{cases} \tag{34}$$

and

$$\begin{aligned} \widetilde{\psi}^{(1)}(z) &:= \tfrac{\partial \widetilde{\varphi}^{(1)}}{\partial z} = \tfrac{\partial \widetilde{T}}{\partial x} - \imath \tfrac{\partial \widetilde{T}}{\partial y} - 1, \qquad z \in D_0, \\ \widetilde{\psi}_k^{(1)}(z) &:= \tfrac{\partial \widetilde{\varphi}_k^{(1)}}{\partial z} = \tfrac{\lambda_m + \lambda_i}{2\lambda_m} \left(\tfrac{\partial \widetilde{T}_k}{\partial x} - \imath \tfrac{\partial \widetilde{T}_k}{\partial y} \right), \quad z \in D_k. \end{aligned} \tag{35}$$

Besides, we mention that when the temperature has a constant jump corresponding to the external field applied in the y-direction

$$\widetilde{T}(z+1) = \widetilde{T}(z), \quad \widetilde{T}(z+\imath) = \widetilde{T}(z) - 1,$$

the temperature is defined as

$$\widetilde{T}(z) = \begin{cases} \operatorname{Re}\left(\widetilde{\varphi}^{(2)}(z) + \imath z\right), \ z \in D_{matrix}, \\ \\ \frac{2\lambda_m}{\lambda_m + \lambda_i} \operatorname{Re} \widetilde{\varphi}_k^{(2)}(z), \ z \in D_{inc}, \end{cases} \tag{36}$$

with corresponding functions $\widetilde{\varphi}^{(2)}, \widetilde{\varphi}_k^{(2)}$ possess the same properties as the functions $\widetilde{\varphi}^{(1)}, \widetilde{\varphi}_k^{(1)}$, and

$$\widetilde{\varphi}^{(2)}(t) = \widetilde{\varphi}_k^{(2)}(t) - \rho \overline{\widetilde{\varphi}_k^{(2)}(t)} - \imath t, \qquad |t - a_k| = R.$$

The corresponding $\mathbb{R}$-linear conjugation boundary value problem has a form

$$\widetilde{\psi}^{(2)}(t) = \widetilde{\psi}_k^{(2)}(t) + \rho \left(\frac{R}{t - a_k} \right)^2 \overline{\widetilde{\psi}_k^{(2)}(t)} - \imath, \quad |t - a_k| = R. \tag{37}$$

The problems (27) and (28) can be reduced to the problems (33) and (37) by the following replacements:

$$\psi^{(1)}(z) = B_1 \widetilde{\psi}^{(1)}(z), \quad \psi_k^{(1)}(z) = B_1 \widetilde{\psi}_k^{(1)}(z), \tag{38}$$

$$\psi^{(2)}(z) = B_2 \widetilde{\psi}^{(2)}(z), \quad \psi_k^{(2)}(z) = B_2 \widetilde{\psi}_k^{(2)}(z). \tag{39}$$

Remark 3.1 *It is easy to verify that the functions* $\widetilde{\psi}^{\perp}(z) := i\widetilde{\psi}^{(2)}(\imath z)$ *and* $\widetilde{\psi}_k^{\perp}(z) := i\widetilde{\psi}_k^{(2)}(\imath z)$ *satisfy the following* $\mathbb{R}$*-linear conjugation boundary value problem*

$$\widetilde{\psi}^{\perp}(t) = \widetilde{\psi}_k^{\perp}(t) + \rho\left(\frac{R}{t-b_k}\right)^2 \overline{\widetilde{\psi}_k^{\perp}(t)} + 1, \quad |t-b_k| = R, \quad b_k = -\imath a_k. \quad (40)$$

Note that $\widetilde{\psi}^{(2)}(z) = -\imath\widetilde{\psi}^{\perp}(-\imath z)$ and $\widetilde{\psi}_k^{(2)}(z) = -\imath\widetilde{\psi}_k^{\perp}(-\imath z)$.

Thus, to find a solution of the problem (26), it is sufficient to find solutions $\widetilde{\psi}^{(1)}(z), \widetilde{\psi}_k^{(1)}(z)$ and $\widetilde{\psi}^{\perp}(z), \widetilde{\psi}_k^{\perp}(z)$ of the problems (33) and (40), respectively.

4 Solution of the problem

First, let us find the real constants B_1 and B_2.

We introduce further notations

$$I := \int\limits_{-\frac{1}{2}}^{\frac{1}{2}} \operatorname{Re}\widetilde{\psi}^{(1)}\Big(\frac{1}{2}+\imath y\Big)\,dy, \quad I^{\perp} := \int\limits_{-\frac{1}{2}}^{\frac{1}{2}} \operatorname{Re}\widetilde{\psi}^{\perp}\Big(\frac{1}{2}+\imath y\Big)\,dy.$$

In general, the integrals I and $I^{\perp}$ differ from zero. As it is shown in Remark 4.3 below

$$\int\limits_{-\frac{1}{2}}^{\frac{1}{2}} \operatorname{Im}\widetilde{\psi}^{(1)}\Big(x+\frac{\imath}{2}\Big)\,dx = 0. \quad (41)$$

Taking $B_2 = 0$ (which corresponds to the problem (27)) and using (15), (18) and (38), we obtain

$$\lambda_m\frac{\partial T(x,\frac{1}{2})}{\partial y} = -\lambda_m \operatorname{Im}\Big(\psi\Big(x+\frac{\imath}{2}\Big)+B\Big) = -\lambda_m B_1 \operatorname{Im}\widetilde{\psi}^{(1)}\Big(x+\frac{\imath}{2}\Big),$$

and

$$\lambda_m\frac{\partial T(\frac{1}{2},y)}{\partial x} = \lambda_m \operatorname{Re}\Big(\psi\Big(\frac{1}{2}+\imath y\Big)+B\Big) = \lambda_m B_1\Big(\operatorname{Re}\big(\widetilde{\psi}^{(1)}\Big(\frac{1}{2}+\imath y\Big)+1\big)\Big).$$

Due to (41), integration on $\left[-\frac{1}{2},\frac{1}{2}\right]$ the first equality gives

$$\lambda_m \int\limits_{-\frac{1}{2}}^{\frac{1}{2}} \frac{\partial T(x,\frac{1}{2})}{\partial y} dx = 0.$$

Integrating on $\left[-\frac{1}{2},\frac{1}{2}\right]$ the second equality and applying (11), we obtain the constant B_1:

$$B_1 = \frac{-A\cos\theta}{\lambda_m(I+1)}. \tag{42}$$

Similarly, taking $B_1 = 0$ (which corresponds to the problem (28)) and using (15), (18) and (38), we obtain

$$\lambda_m \frac{\partial T(x,\frac{1}{2})}{\partial y} = -\lambda_m \mathrm{Im}\left(\psi\Big(x+\frac{\imath}{2}\Big)+B\right) = -\lambda_m B_2 \mathrm{Im}\left(\widetilde{\psi}^{(2)}\Big(x+\frac{\imath}{2}\Big)\right) - \lambda_m B_2,$$

and

$$\lambda_m \frac{\partial T(\frac{1}{2},y)}{\partial x} = \lambda_m \mathrm{Re}\left(\psi\Big(\frac{1}{2}+\imath y\Big)+B\right) = \lambda_m B_2 \mathrm{Re}\left(\widetilde{\psi}^{(2)}\Big(\frac{1}{2}+\imath y\Big)\right).$$

Using the equality $\widetilde{\psi}^{(2)}(z) = -\imath\widetilde{\psi}^{\perp}(-\imath z)$, we have

$$\mathrm{Im}\left(\widetilde{\psi}^{(2)}\Big(x+\frac{\imath}{2}\Big)\right) = -\mathrm{Re}\left(\widetilde{\psi}^{\perp}\Big(\frac{1}{2}-\imath x\Big)\right),$$

$$\mathrm{Re}\left(\widetilde{\psi}^{(2)}\Big(\frac{1}{2}+\imath y\Big)\right) = \mathrm{Im}\left(\widetilde{\psi}^{\perp}\Big(-\frac{\imath}{2}+y\Big)\right).$$

Thus, we get

$$\lambda_m \int\limits_{-\frac{1}{2}}^{\frac{1}{2}} \frac{\partial T(\frac{1}{2},y)}{\partial x} dy = 0.$$

Integrating on $\left[-\frac{1}{2},\frac{1}{2}\right]$ the term $\lambda_m \frac{\partial T(x,\frac{1}{2})}{\partial y}$ and applying (10), we obtain the constant B_2:

$$B_2 = \frac{-A\sin\theta}{\lambda_m(I^{\perp}-1)}. \tag{43}$$

Taking into the account the properties of functions under consideration from Sections 2 and 3, the results obtained above and Remark 3.1, we arrive at the following theorem:

Theorem 4.1 *Let $T = T(x, y)$ and $T_k = T_k(x, y)$ be the solution of the problem (6)-(7), (10) and (11). The temperature flux is defined in the following form:*

$$\frac{\partial T(x,y)}{\partial x} - \imath \frac{\partial T(x,y)}{\partial y} = \begin{cases} \psi(z) + B, \ z = x + \imath y \in D_{matrix}, \\ \\ \frac{2\lambda_m}{\lambda_m + \lambda_i} \psi_k(z), \ z = x + \imath y \in D_{inc}, \end{cases} \tag{44}$$

where

$$B = \frac{-A\cos\theta}{\lambda_m(I+1)} - \frac{A\sin\theta}{\lambda_m(I^{\perp}-1)}\,\imath,$$

and

$$\psi(z) := \frac{-A\cos\theta}{\lambda_m(I+1)}\widetilde{\psi}^{(1)}(z) + \imath\frac{A\sin\theta}{\lambda_m(I^{\perp}-1)}\widetilde{\psi}^{\perp}(-\imath z), \ z \in D_{matrix},$$

$$\psi_k(z) := \frac{-A\cos\theta}{\lambda_m(I+1)}\widetilde{\psi}_k^{(1)}(z) + \imath\frac{A\sin\theta}{\lambda_m(I^{\perp}-1)}\widetilde{\psi}_k^{\perp}(-\imath z), \ z \in D_{inc}.$$

To find the temperature, it is sufficient to find the functions $\varphi, \varphi_1, \ldots, \varphi_N$ (cf. (15)). These functions can be represented as sums $\varphi(z) = \varphi^{(1)}(z) + \varphi^{(2)}(z)$, $\varphi_k(z) = \varphi_k^{(1)}(z) + \varphi_k^{(2)}(z)$ of two functions $\varphi^{(1)}$ and $\varphi^{(2)}$ have to satisfy the following BVPs:

$$\varphi^{(1)}(t) = \varphi_k^{(1)}(t) - \rho\overline{\varphi_k^{(1)}(t)} - B_1 t, \tag{45}$$

$$\varphi^{(2)}(t) = \varphi_k^{(2)}(t) - \rho\overline{\varphi_k^{(2)}(t)} - \imath B_2 t. \tag{46}$$

Analogously to (38)–(39), we have $\varphi^{(1)}(z) = B_1\widetilde{\varphi}^{(1)}(z)$, $\varphi_k^{(1)}(z) = B_1\widetilde{\varphi}_k^{(1)}(z)$ and $\varphi^{(2)}(z) = B_2\widetilde{\varphi}^{(2)}(z)$, $\varphi_k^{(2)}(z) = B_2\widetilde{\varphi}_k^{(2)}(z)$. It is easy to verify that

$$\widetilde{\varphi}^{(2)}(z) = \widetilde{\varphi}^{(1)}(-\imath z), \ \widetilde{\varphi}_k^{(2)}(z) = \widetilde{\varphi}_k^{(1)}(-\imath z).$$

The functions $\widetilde{\varphi}^{(1)}$ and $\widetilde{\varphi}_k^{(1)}$ can be found up to an arbitrary constant as indefinite integrals of the functions $\widetilde{\psi}^{(1)}$ and $\widetilde{\psi}_k^{(1)}$, respectively (cf. (35)). Thus, we arrive at the following statement:

Theorem 4.2 *Let $T = T(x, y)$ and $T_k = T_k(x, y)$ be the solution of the problem (6)-(7), (10) and (11). The temperature distribution can be found up to an arbitrary constant and is defined in the form (15), where*

$$B = \frac{-A\cos\theta}{\lambda_m(I+1)} - \frac{A\sin\theta}{\lambda_m(I^{\perp}-1)}\,\imath,$$

$$\varphi(z) = \frac{-A\cos\theta}{\lambda_m(I+1)}\widetilde{\varphi}^{(1)}(z) - \frac{A\sin\theta}{\lambda_m(I^{\perp}-1)}\widetilde{\varphi}^{(1)}(-\imath z),$$
$$\varphi_k(z) = \frac{-A\cos\theta}{\lambda_m(I+1)}\widetilde{\varphi}_k^{(1)}(z) - \frac{A\sin\theta}{\lambda_m(I^{\perp}-1)}\widetilde{\varphi}_k^{(1)}(-\imath z).$$

Now we describe a new algorithm for solution of the problem (33). The problem (40) can be solved analogously. For convenience, we omit upper index in $\widetilde{\psi}^{(1)}$ and will write $\widetilde{\psi}$ below. We shortly describe solvability of the problem (33) using some facts and notation of the paper [4].

Notice that we have N contours ∂D_k and N complex conjugation conditions on each contour ∂D_k but we need to find $N+1$ functions $\widetilde{\psi}, \widetilde{\psi}_1, \ldots, \widetilde{\psi}_N$. This means that we need one additional condition to close up the system. For this reason we introduce a new doubly periodic function Φ which is a sectionally analytic in $Q_{(0,0)}$ and in $\bigcup\limits_{k=1}^{N} D_k$ and has the zero jumps along each ∂D_k, $k = 1, 2, \ldots, N$. Such consideration will give an additional condition on $\widetilde{\psi}, \widetilde{\psi}_1, \ldots, \widetilde{\psi}_N$. We will show that $\Phi \equiv 0$.

Let us introduce the sectionally analytic doubly periodic function Φ by the following formula:

$$\Phi(z) = \begin{cases} \widetilde{\psi}_k(z) - \rho \sum\limits_{m=1}^{N} {\sum\limits_{m_1,m_2}}^{*} W_{m_1,m_2,m}\widetilde{\psi}_m(z) - 1, \ |z-a_k| \le R, \\ \widetilde{\psi}(z) - \rho \sum\limits_{m=1}^{N} \sum\limits_{m_1,m_2} W_{m_1,m_2,m}\widetilde{\psi}_m(z), \ z \in D_0, \end{cases} \tag{47}$$

where

$$W_{m_1,m_2,m}\widetilde{\psi}_m(z) = \left(\frac{R}{z-a_m-m_1-\imath m_2}\right)^2 \overline{\widetilde{\psi}_m\left(\frac{R^2}{z-a_m-m_1-\imath m_2}+a_m\right)} \tag{48}$$

and

$$\sum_{m=1}^{N} {\sum_{m_1,m_2}}^{*} W_{m_1,m_2,m} := \sum_{m\neq k} \sum_{m_1,m_2} W_{m_1,m_2,m} + {\sum_{m_1,m_2}}' W_{m_1,m_2,k}. \tag{49}$$

The "prime" notation in ${\sum\limits_{m_1,m_2}}'$ means that the summation occurs in all m_1 and m_2 except at $(m_1, m_2) = (0, 0)$.

Applying *Analytic Continuation Principle* and *Liouville's* theorem for doubly periodic functions, we have that $\Phi = c$.

Let $\widetilde{\psi}$ and $\widetilde{\psi}_k$ be solutions of the system $\Phi(z) = c$. Then, in D_0, we have

$$\widetilde{\psi}(z) = \widetilde{\psi}'(z) + c \tag{50}$$

with some doubly periodic function $\widetilde{\psi}'$. Inserting the last equality in (35) and then in (30), we obtain

$$T(z) = \mathrm{Re}\,(\widetilde{\varphi}'(z) + cz + z), \quad z \in D_0, \tag{51}$$

with some function $\widetilde{\varphi}'$ which yields $c = 0$. Thus, we have $\Phi(z) \equiv 0$. Writing $\Phi(z) \equiv 0$, we obtain the following system of linear functional equations

$$\widetilde{\psi}_k(z) = \rho \sum_{m=1}^{N} {\sum_{m_1,m_2}}^{*} W_{m_1,m_2,m} \widetilde{\psi}_m(z) + 1 \tag{52}$$

which is uniquely solvable with respect to $\widetilde{\psi}_k$ in the space of analytical functions (for more details cf. [4]).

The function $\widetilde{\psi}$ has the form

$$\widetilde{\psi}(z) = \rho \sum_{m=1}^{N} \sum_{m_1,m_2} W_{m_1,m_2,m} \widetilde{\psi}_m(z). \tag{53}$$

Let us expand $\widetilde{\psi}_k(z)$ into Taylor series

$$\widetilde{\psi}_k(z) = \sum_{l=0}^{\infty} \widetilde{\psi}_{lk} (z - a_k)^l \tag{54}$$

in order to sum up $W_{m_1,m_2,k}\widetilde{\psi}_k(z)$ over all translations $m_1 + \imath m_2$.

The series $\sum\limits_j W_{j,k}\widetilde{\psi}_k(z)$, where $j = (m_1, m_2)$ and k is a fixed number, can be represented via the elliptic Eisenstein functions $E_l(z)$ of order l (see [27]):

$$\sum_j W_{j,k}\widetilde{\psi}_k(z) = \sum_{l=0}^{\infty} \overline{\widetilde{\psi}_{lk}} R^{2(l+1)} E_{l+2}(z - a_k). \tag{55}$$

The series $\sum\limits_j{}' W_{j,k}\widetilde{\psi}_k(z) := \sum\limits_j W_{j,k}\widetilde{\psi}_k(z) - \left(\frac{R}{z-a_k}\right)^2 \overline{\widetilde{\psi}_k\left(\frac{R^2}{z-a_k} + a_k\right)}$ can be written in the form

$$\sum_j{}' W_{j,k}\widetilde{\psi}_k(z) = \sum_{l=0}^{\infty} \overline{\widetilde{\psi}_{lk}} R^{2(l+1)} \sigma_{l+2}(z - a_k), \tag{56}$$

where σ_l is the modified Eisenstein function defined by the formula $\sigma_l(z) := E_l(z) - z^{-l}$. The Eisenstein functions E_l converges absolutely and uniformly for $l = 3, 4, \ldots$ and conditionally for $l = 2$ ([27]).

Thus, we can rewrite the equations (52) and (53) for $\widetilde{\psi}_k$ and $\widetilde{\psi}$ as follows:

$$\widetilde{\psi}_k(z) = \rho \sum_{m \neq k}^{N} \sum_{l=0}^{\infty} \overline{\widetilde{\psi}_{lm}}\, R^{2(l+1)}\, E_{l+2}(z - a_m) + \rho \sum_{l=0}^{\infty} \overline{\widetilde{\psi}_{lk}}\, R^{2(l+1)}\, \sigma_{l+2}(z - a_k) + 1, \tag{57}$$

$$\widetilde{\psi}(z) = \rho \sum_{m=1}^{N} \sum_{l=0}^{\infty} \overline{\widetilde{\psi}_{lm}}\, R^{2(l+1)}\, E_{l+2}(z - a_m). \tag{58}$$

Now we need to find the numerical coefficients $\widetilde{\psi}_{lm}$ of the system (57). Note that the equation (58) for $\widetilde{\psi}$ has the same coefficients $\widetilde{\psi}_{lm}$. Taking a partial sum of Taylor series with M first items

$$\widetilde{\psi}_k(z) = \widetilde{\psi}_{0k} + \widetilde{\psi}_{1k}(z - a_k) + \widetilde{\psi}_{2k}(z - a_k)^2 + \cdots + \widetilde{\psi}_{Mk}(z - a_k)^M$$

and collecting the coefficients of the like powers of $z - a_k$, we obtain the formula for definition of $\widetilde{\psi}_{jk}$:

$$\widetilde{\psi}_{jk} = \frac{1}{j!} \widetilde{\psi}_k^{(j)} \Big|_{z = a_k}, \tag{59}$$

where $\widetilde{\psi}_k^{(j)}$ is derivative of order j of the function $\widetilde{\psi}_k$. Then, we get

$$\widetilde{\psi}_{jk} = \frac{\rho}{j!} \sum_{m \neq k}^{N} \sum_{l=0}^{M} \overline{\widetilde{\psi}_{lm}} R^{2(l+1)} (-1)^j \frac{(l + j + 1)!}{(l + 1)!} E_{l+j+2}(a_k - a_m)$$

$$+ \frac{\rho}{j!} \sum_{l=0}^{M} \overline{\widetilde{\psi}_{lk}} R^{2(l+1)} (-1)^j \frac{(l + j + 1)!}{(l + 1)!} \sigma_{l+j+2}(0) + I_j, \tag{60}$$

where $I_j = \begin{cases} 1, \ j = 0, \\ 0, \ j = 1, \ldots, M. \end{cases}$

Thus, we arrive at the system with $N(M+1)$ unknown constants $\widetilde{\psi}_{jk}$ and $N(M+1)$ equations which can be solved numerically. Note that this system is obtained for an arbitrary number N of inclusions.

Remark 4.3 *Note that doubly periodicity of* E_{l+2} *and the relations* $E'_{l+2} = -(l+2)E_{l+3}$, $l = 0, 1, 2, \ldots$ *imply* $\int\limits_{-0.5}^{0.5} E_{l+2}(x + 0.5\imath)\, dx = 0$ *for* $l = 1, 2, \ldots,$ *while the equality* $\int\limits_{-0.5}^{0.5} E_2(x + 0.5\imath)\, dx = 0$ *can be obtained by numerical calculation. Therefore,* $\int\limits_{-0.5}^{0.5} \widetilde{\psi}(x + 0.5\imath)\, dx = 0.$

Remark 4.4 *Note that for finding of the flux distribution (namely, the functions* $\widetilde{\psi}, \widetilde{\psi}_k, \ldots, \widetilde{\psi}_N$*) in an explicit form, we change an algorithm of solution of the equations (57) and (58) in comparison with the algorithm represented in [4]. It allows to get more accurate numerical values of the flux in each point of considered composite material.*

Remark 4.5 *Note that it is possible to find the heat flux distribution in each cell* $Q_{(m_1,m_2)}$ *with corresponding centers* $a_1 + m_1 + \imath m_2$, $a_2 + m_1 + \imath m_2$, $a_3 + m_1 + \imath m_2$, $a_4 + m_1 + \imath m_2$.

Thus in the next section when discussing numerical results we are concentrating only on the computations in the $Q_{(0,0)}$ unit cell.

5 Numerical results and discussions

5.1 Accuracy of the computations

The new algorithm to solve numerically obtained system is realized in Maple 14 software. As an example, we consider the case when four inclusions are situated within one cell, i.e., $N = 4$. We suppose throughout the computations that the heat flux of the fixed intensity $A = -1$ flows in different directions with respect to the main axis. Here the minus sign shows that the flux is directed from the right to the left (or from the top to the bottom) depending on the angle θ. The conductivity of the matrix is set as $\lambda_m = 1$, while those for the inclusions, λ_i, will take different values.

First we analyze the accuracy of the computations when using the modified algorithm described in (57) – (60).

We take for our tests a non-symmetrical configuration, with respect to Ox-axis, with two inclusions situated close enough to each other as depicted

Table 1: Basic parameters computed for $M = 4$ iterations. Centers of the inclusions (the same radii $R = 0.145$) are defined in (61).

θ	B_1	B_2	$\int_{-1/2}^{1/2} q_1(\xi)d\xi$	$\int_{-1/2}^{1/2} q_2(\xi)d\xi$
$\lambda_i = 0.001$				
0	1.867004	0	$-9.9 \cdot 10^{-7}$	$-3.3 \cdot 10^{-16}$
$\pi/2$	0	-1.652566	$2.5 \cdot 10^{-12}$	$2.8 \cdot 10^{-8}$
$\pi/4$	1.320171	-1.168540	$-7.0 \cdot 10^{-6}$	$2.0 \cdot 10^{-8}$
$\lambda_i = 0.01$				
0	1.840595	0	$-9.3 \cdot 10^{-6}$	$2.2 \cdot 10^{-16}$
$\pi/2$	0	-1.637998	$5.5 \cdot 10^{-12}$	$2.2 \cdot 10^{-8}$
$\pi/4$	1.301497	-1.158240	$-6.6 \cdot 10^{-6}$	$1.6 \cdot 10^{-8}$
$\lambda_i = 0.1$				
0	1.6301608	0	$-5.3 \cdot 10^{-6}$	$-1.1 \cdot 10^{-16}$
$\pi/2$	0	-1.511547	$1.95 \cdot 10^{-12}$	$-1.1 \cdot 10^{-8}$
$\pi/4$	1.1526977	-1.068825	$-3.7 \cdot 10^{-6}$	$-8.1 \cdot 10^{-9}$
$\lambda_i = 1$				
0	1	0	0	$2.2 \cdot 10^{-16}$
$\pi/2$	0	-1	$2.2 \cdot 10^{-16}$	0
$\pi/4$	0.7071068	-0.7071068	$-1.1 \cdot 10^{-16}$	$-1.1 \cdot 10^{-16}$
$\lambda_i = 10$				
0	0.66154467	0	$-1.3 \cdot 10^{-6}$	$2.2 \cdot 10^{-16}$
$\pi/2$	0	-0.61309308	$-4.8 \cdot 10^{-13}$	$-3.9 \cdot 10^{-7}$
$\pi/4$	0.46778272	-0.43352227	$-9.1 \cdot 10^{-7}$	$-2.8 \cdot 10^{-7}$
$\lambda_i = 100$				
0	0.61045509	0	$-1.7 \cdot 10^{-6}$	$2.2 \cdot 10^{-16}$
$\pi/2$	0	-0.54238833	$-6.2 \cdot 10^{-13}$	$-6.7 \cdot 10^{-7}$
$\pi/4$	0.43165693	-0.38352646	$-1.2 \cdot 10^{-6}$	$-4.7 \cdot 10^{-7}$
$\lambda_i = 1000$				
0	0.605071574	0	$-1.7 \cdot 10^{-6}$	0
$\pi/2$	0	-0.53460516	$-3.1 \cdot 10^{-12}$	$-7.0 \cdot 10^{-7}$
$\pi/4$	0.42785021	-0.37802293	$-1.2 \cdot 10^{-6}$	$-5.0 \cdot 10^{-7}$

on Fig. 2. The centers of the inclusions are situated in the points:

$$a_1 = -0.18+0.2\imath, \quad a_2 = 0.33-0.34\imath, \quad a_3 = 0.33+0.35\imath, \quad a_4 = -0.18-0.2, \tag{61}$$

while their radii are the same $R_i = R$. Note that two inclusions from the neighboring cells are situated very close to each other. Thus it is impossible to neglect the interactions between them.

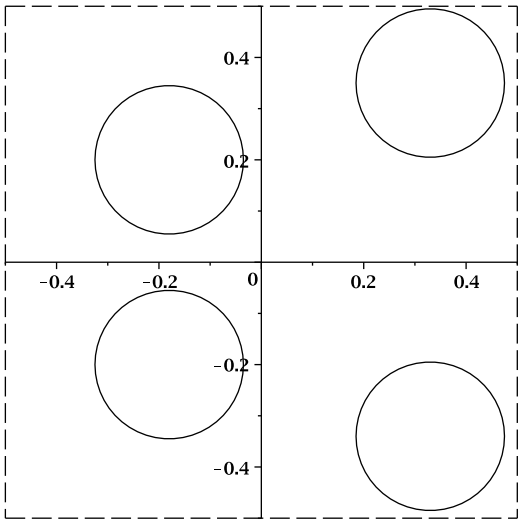

Figure 2: The cell $Q_{(0,0)}$.

The results of the analysis for different contrast ρ between the materials of matrix and the inclusions are presented in Table 1. The results indicate that the maximal error in the computations was on the level of 10^{-6} or better. As an indirect measures we use here the integrals of the auxiliary functions q_j showing deviation of the flux within each unit cell from its uniform distribution. All these values should be zeros as follows from (12). Other computations below suggest that accuracy of the flux components guarantees five valid digits.

Remark 5.1 *Additional computations performed by us show that for relatively large values of the radius, an accuracy depends on the positions of the inclusions. More symmetric configurations with respect to any axis provide better accuracy. For an arbitrary (nonsymmetric) configurations, a higher accuracy is achieved for smaller radiuses of inclusions.*

The flux components Q_x and Q_y in the center a_k of k-inclusion

$$Q_x^{(k)}(a_k) \equiv \lambda_k \frac{\partial T_k(a_k)}{\partial x} = \frac{2\lambda_k\lambda_m}{\lambda_m + \lambda_k} \cdot \mathrm{Re}\,\psi_k(a_k),$$

$$Q_y^{(k)}(a_k) \equiv \lambda_k \frac{\partial T_k(a_k)}{\partial y} = -\frac{2\lambda_k\lambda_m}{\lambda_m + \lambda_k} \cdot \mathrm{Im}\,\psi_k(a_k),$$

are calculated in accordance with the formula (44). The flux components in any point of the matrix can be found as

$$Q_x^{(m)}(z) = \lambda_m \cdot \mathrm{Re}\,(\psi(z) + B), \quad Q_y^{(m)}(z) = -\lambda_m \cdot \mathrm{Im}\,(\psi(z) + B).$$

We calculate $Q_x^{(m)}(z)$ and $Q_y^{(m)}(z)$ at the point $z = 0 \in D_{matrix}$ belonging to the matrix. Computations in the Table 2 are given for four consequent iterations ($M = 1, ..., 4$), and fixed other parameters: $\theta = 0$, $R = 0.135$, $\lambda_m = 1$, $\lambda_i = 100$. Note that the accuracy (five valid digits) predicted from the computations in the Table 1 has been confirmed also from other analysis below. Note that the convergence is not monotonous as the consequent terms in the series change their signs.

Table 2: The flux components for different iterations M, while other problem parameters are: $\theta = 0$, $R = 0.135$, $\lambda_m = 1$, $\lambda_i = 100$ and the configurations of inclusion defined by (61).

M	$Q_x^{(1)}(a_1)$	$Q_y^{(1)}(a_1)$	$Q_x^{(m)}(0)$	$Q_y^{(m)}(0)$
0	1.553864	−0.005491	0.779414	−0.0015248
1	1.561173	−0.005155	0.769965	−0.0016577
2	1.561668	−0.005273	0.764487	−0.0016911
3	1.561562	−0.005274	0.764280	−0.0016916
4	1.561566	−0.005275	0.764289	−0.0016913

One can observe form the table that the computational accuracy is between five or six valid units depending on where the flux is computed. Note that the material contract is rather high thus the accuracy is good enough inside both the materials (in the matrix and in the inclusions).

5.2 Average properties of the composite

The effective conductivity of microscopically isotropic composite materials with a small concentration $\nu = N\pi R^2 \ll 1$ of periodic inclusions is defined by the spherical tensor $\Lambda_e = \lambda_e \mathbf{I}$ where the effective conductivity is computed by the classical Clausius-Mossotti formula

$$\lambda_e = \lambda_m \cdot \frac{1+\rho\nu}{1-\rho\nu} + \mathcal{O}(\nu^2), \quad \nu \to 0, \tag{62}$$

where $\rho = (\lambda_i - \lambda_m)/(\lambda_i + \lambda_m)$. For the history and applications of this formula see for example [19].

In general case of composites with random non-overlapping inclusions the tensor of effective conductivity Λ_e has a form

$$\Lambda_e = \begin{pmatrix} \lambda_e^x & \lambda_e^{xy} \\ \lambda_e^{yx} & \lambda_e^y \end{pmatrix} \tag{63}$$

with components obtained in [4] in the case when the temperature has a unit jump along Ox-axis (see (29)) in the following manner:

$$\widetilde{\lambda}_e^x - \imath\widetilde{\lambda}_e^{xy} = \lambda_m(1 + 2\rho\nu\widetilde{\Psi}), \tag{64}$$

where parameter Ψ depends on the material contrast, ρ, density of the inclusions, ν, and their positions in the cell:

$$\widetilde{\Psi} = \widetilde{\Psi}(\rho, \nu, a_j) = \frac{1}{N}\sum_{j=1}^{N} \widetilde{\psi}_j(a_j). \tag{65}$$

Using (57) one can prove that for any fixed ρ and for any non symmetrical distribution of the inclusions, the following estimate is true

$$\widetilde{\Psi}(\rho, \nu, a_j) = 1 + \mathcal{O}(\nu), \quad \nu \to 0.$$

Thus, the formula (62) coincides with (64) with an accuracy of $\mathcal{O}(\nu^2)$ for $\theta = 0$ and $\theta = \pi/2$. Another conclusion which immediately follows from this preliminary analysis is that the next asymptotic term in the formula (62) should depend on the positions of the inclusions.

The effective conductivity in the direction of the coordinate system can be found in the form (see Appendix 1):

$$\lambda_e^x(\theta) - \imath\lambda_e^y(\theta) = -A\lambda_m e^{-\imath\theta} + \frac{2\lambda_m\rho\nu}{N}\sum_{k=1}^{N} \psi_k(\theta, a_k) \tag{66}$$

for an arbitrary direction of the heat flow propagating in the composite and defined by the angle θ. Note that in case of $\theta = 0$ and $A = -1$ it coincides with the formula (64).

To compare the results obtained on the base of the improved algorithm and the classical Clausius-Mossotti formula in values we choose a periodic array of four inclusions ($N = 4$) placed symmetrically in the unit cell with the centers: $a_1 = -0.25 + 0.25\imath$, $a_2 = 0.25 + 0.25\imath$, $a_3 = 0.25 - 0.25\imath$, $a_4 = -0.25 - 0.25\imath$. Other parameters are: the flux flows along Ox-axis ($\theta = 0$), $A = -1$, inclusions conductivities $\lambda_i = 100$ and various values of the concentration parameter ν. We find the effective conductivity using formula (66) by the new algorithms computed the values of function $\psi_i(a_i)$ (the imposed symmetry leads to $\lambda_e = \lambda_e^x$, $\lambda_e^{xy} = 0$). In Table 3, a comparison of results calculated by two methods is presented.

Table 3: Comparison of the effective conductivities λ_e computed by the new algorithm and the classic Clausius-Mossotti formula λ_e^{CM}. Here the value $\delta\lambda = (\lambda_e^{CM} - \lambda_e)/\lambda_e$ indicates the accuracy of the approximate formula.

R	ν	D/d	λ_e^{CM}	λ_e	$\frac{\lambda_e^{CM}-\lambda_e}{\nu^2}$	$\delta\lambda$
0	0	0	1	1	–	0
0.005	0.0204	0.00031	1.00061607	1.00061569	3.84021	$3.8 \cdot 10^{-7}$
0.03	0.01131	0.1364	1.02242010	1.021928	3.84362	$4.8 \cdot 10^{-4}$
0.07	0.06158	0.3889	1.12846546	1.11384	3.85708	$1.3 \cdot 10^{-2}$
0.1	0.12566	0.6667	1.28095768	1.21935	3.90145	$5.1 \cdot 10^{-2}$
0.12	0.18095	0.9231	1.43123393	1.30138	3.96553	$1.0 \cdot 10^{-1}$

Note that computations for $\nu = 0.0204$ exhibits much better accuracy that reported in the Tables 1 and 2. This fact has been explained in the Remark 5.1. Simultaneously, the classic formula provides the results with the relative accuracy of 10^{-7}. On the contrary, the value $\nu = 0.18095$ in our computations stands for rather high inclusions concentration than low. Indeed, one can see that in this case the inclusion diameter, $D = 0.24$, and the distance between the inclusions, $d = 0.26$, are comparable in values. From the results presented in the table one can extract the constant in the estimate $\mathcal{O}(\nu^2)$ from (62) and the relative error between the classic and the exact formulas. As follows from the computation to have the deviation between

the formulas less that 1% the distance between the inclusions should be larger than their diameters at least two times. Clearly, the results refer to the particular chosen configuration of inclusions and the contrast parameter ρ.

Now we return back to the original asymmetric configuration (61). The new algorithm allows us to defined the tensor of effective conductivity for the case too. The components λ_e^x and λ_e^{xy} are calculated using the formula (66). The components λ_e^y and λ_e^{yx} of the tensor (63) should be calculated in the similar manner by choosing the orthogonal direction of the flux. We use for the computations the materials conductivities $\lambda_i = 100$, $\lambda_m = 1$. Values of all components of the tensor Λ_e as functions on the concentration ν are presented for different angles in Table 4.

Table 4: The components of the effective conductivity tensor Λ_e for the configuration of the inclusions given in (61) for the material constants $\lambda_i = 100$ and $\lambda_m = 1$.

R	λ_e^x	λ_e^{xy}	λ_e^y	λ_e^{yx}	$\lambda_e^x(\pi/8)$	$\lambda_e^{xy}(\pi/8)$
0	1	0	0	1	0.923880	0.382683
0.05	1.059136	$2.2 \cdot 10^{-7}$	1.060379	$2.2 \cdot 10^{-7}$	0.978514	0.405790
0.11	1.249047	$4.4 \cdot 10^{-6}$	1.272899	$4.4 \cdot 10^{-6}$	1.153971	0.487121
0.135	1.348160	$1.1 \cdot 10^{-5}$	1.398658	$1.1 \cdot 10^{-5}$	1.245542	0.535253
0.145	1.389545	$1.5 \cdot 10^{-5}$	1.457632	$1.5 \cdot 10^{-5}$	1.283778	0.557826

Thus the composite described by such configuration of the inclusions is not isotropic. Fig. 2 gives an idea why this should be in the case as the inclusions are placed in the same line if the flux flows vertically while their centers are shifted against each other in horizontal direction. Using the tensorial rule we additionally checked our computations by computing the conductivity of the composite when the flux is directed by the angle $\theta = \pi/8$. The accuracy of the computations using the conductivity tensor Λ_e and the tensorial rule versus the formula (66) was between 10^{-8} and 10^{-6} decreasing with the radius growth.

5.3 The flux and the temperature distribution

As an example, we also show the flux distribution inside the cell $Q_{(0,0)}$ for different angles and conductivities of inclusions on Fig. 3-4. We take for calculations the centers of inclusions in the points (61) and the radius $R = 0.145$.

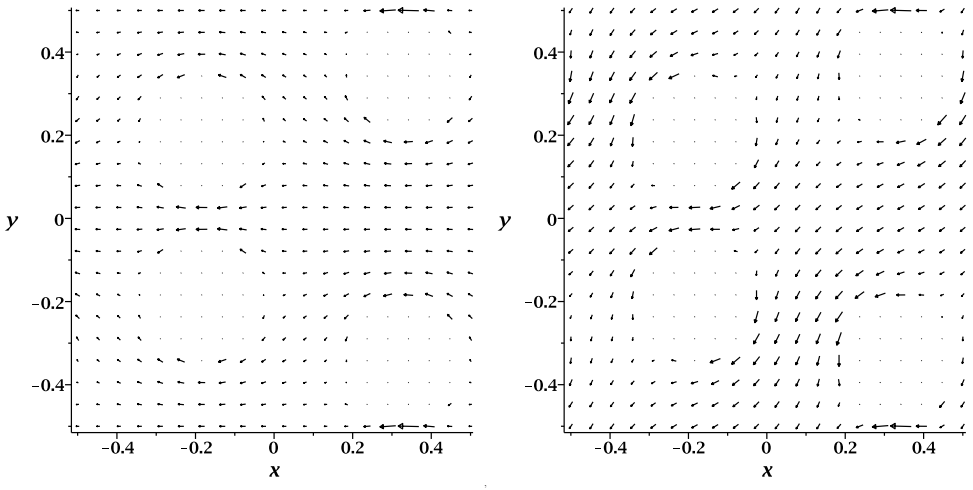

Figure 3: The flux distribution inside $Q_{(0,0)}$ for $\lambda_i = 0.01$, $\theta = 0; \pi/4$.

According to (15) in order to find the temperature function $T = T(x, y)$, one needs to find functions φ and φ_k, $k = 1, \ldots, N$. Using (18) one can recover it, up to arbitrary constant, integrating functions ψ and ψ_k, $k = 1, \ldots, N$. To define the constant, we use the boundary conditions (24). As a result of the integration, Weierstrass zeta-function appears (cf. Appendix 2). The temperature distribution $T(x, y)$ is presented on Fig. 5-6. The same two composite configuration as for the flux distribution are given. Namely, we consider the following set of the parameters: $\lambda_m = 1$, $R = 0.145$, $\theta = 0; \frac{\pi}{4}$ with $\lambda_i = 100$ and $\lambda_i = 0.01$.

To conclude the paper, we have proposed here the improved algorithm to solve the system (47). It allows one to reconstruct the solution and its gradient at an arbitrary point of the composite with an extremely high accuracy even for a few numbers of the iteration points $M = 4$. The constructed algorithm is equally effective in finding the average properties of the composite. We have shown its effectiveness on several examples and discussed

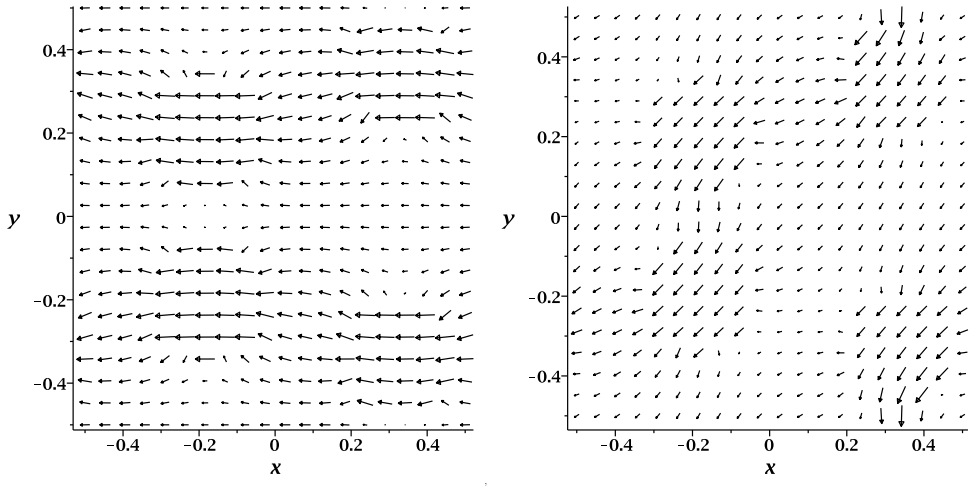

Figure 4: The flux distribution inside $Q_{(0,0)}$ for $\lambda_i = 100$, $\theta = 0; \pi/4$.

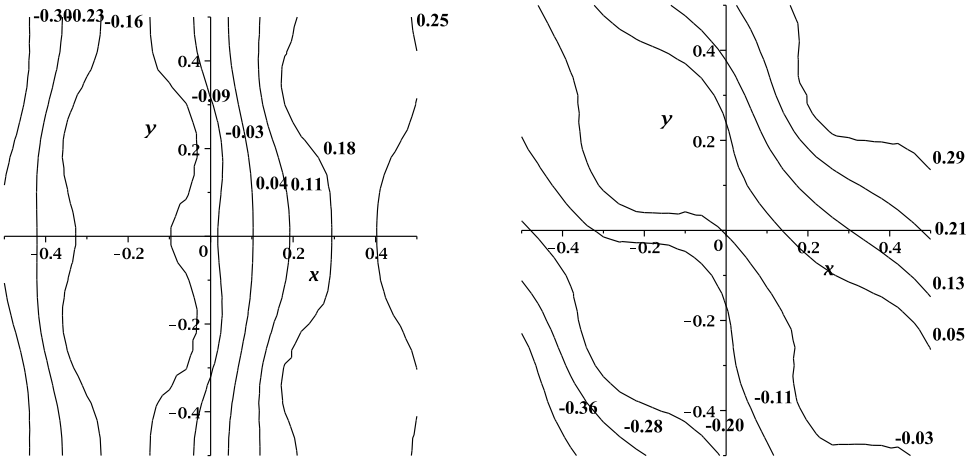

Figure 5: The temperature distribution inside $Q_{(0,0)}$ for $\lambda_i = 100$, $\theta = 0; \pi/4$.

peculiarities of the computations related to a particular configuration of the inclusions. And last but not least, the algorithm constructed in this paper may be used to compute practically arbitrary configurations of the composite while the respective solution (both its local and average values) may be used as benchmarks to test other numerical algorithms.

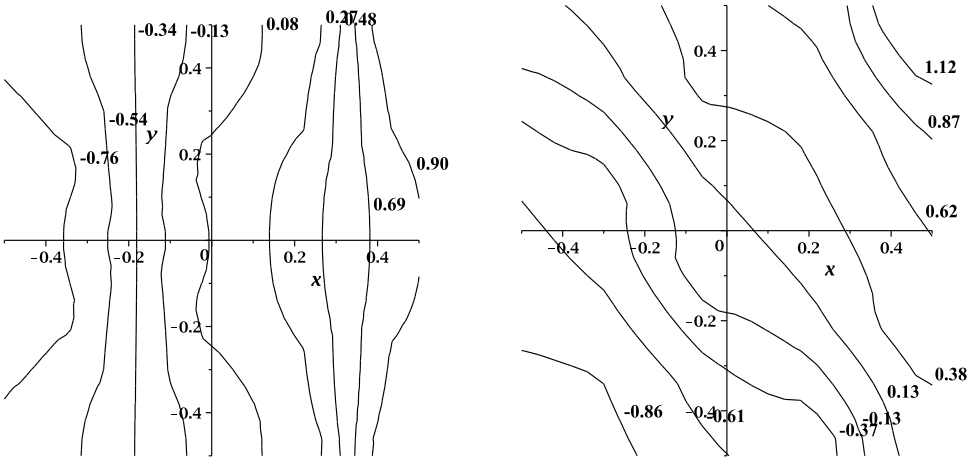

Figure 6: The temperature distribution inside $Q_{(0,0)}$ for $\lambda_i = 0.01$, $\theta = 0; \frac{\pi}{4}$.

5.4 Appendix 1: Evaluation of the effective conductivity.

The effective conductivity in x-direction can be defined by Green's formula as

$$\lambda_e^x(\theta) = \lambda_m \iint\limits_{D_0} \frac{\partial T}{\partial x}\, dxdy + \lambda_i \sum_{k=1}^{N} \iint\limits_{D_k} \frac{\partial T_k}{\partial x}\, dxdy. \tag{67}$$

Using first Green's formula

$$\int_U (\psi \Delta\varphi + \nabla\varphi \cdot \nabla\psi)\, dV = \oint_{\partial U} \psi\, (\nabla\varphi \cdot \mathbf{n})\, dS \tag{68}$$

with $\psi = x$ and $\varphi(x, y) = T$ in D_0 (or $\varphi(x, y) = T_k$ in the respective domain D_k) and taking into account (6) we have

$$\oint_{\partial D_0} x\frac{\partial T}{\partial n} ds = \oint_{\partial Q_{(0,0)}} x\frac{\partial T}{\partial n} ds - \sum_{k=1}^{N} \oint_{\partial D_k} x\frac{\partial T_k}{\partial n} ds, \tag{69}$$

where the curves $\partial Q_{(0,0)}$ and ∂D_k are oriented in the counterclockwise direction.

Here we take into account that the contour integrals along the common boundaries ∂D_k annihilate according to (8). Last integral can be computed

with use of (10) and (11)

$$\iint\limits_{Q_{(0,0)}} \frac{\partial T}{\partial x} dxdy = \oint\limits_{\partial Q_{(0,0)}} x \frac{\partial T}{\partial n} ds = \int_{-1/2}^{1/2} x(-A\sin\theta)dx - \int_{-1/2}^{1/2} x(-A\sin\theta)dx +$$

$$\frac{1}{2}\int_{-1/2}^{1/2}(-A\cos\theta)dy + \frac{1}{2}\int_{-1/2}^{1/2}(-A\cos\theta)dy = -A\cos\theta.$$

In the y-direction, we have

$$\lambda_e^y(\theta) = \lambda_m \iint\limits_{D_0} \frac{\partial T}{\partial y}\, dxdy + \lambda_i \sum_{k=1}^{N} \iint\limits_{D_k} \frac{\partial T_k}{\partial y}\, dxdy. \tag{70}$$

Repeating the same line of the reasoning with $\psi = y$ and $\varphi(x,y) = T$ in D_0 (or $\varphi(x,y) = T_k$ in the respective domain D_k) with first Green's formula (68)

$$\iint\limits_{Q_{(0,0)}} \frac{\partial T}{\partial y}\, dxdy = -A\sin\theta. \tag{71}$$

Thus, we have

$$\iint\limits_{D_0} \frac{\partial T}{\partial x}\, dxdy = -A\cos\theta - \sum_{k=1}^{N} \iint\limits_{D_k} \frac{\partial T_k}{\partial x}\, dxdy,$$

$$\iint\limits_{D_0} \frac{\partial T}{\partial y}\, dxdy = -A\sin\theta - \sum_{k=1}^{N} \iint\limits_{D_k} \frac{\partial T_k}{\partial y}\, dxdy.$$

Then,

$$\lambda_e^x - \imath\lambda_e^y = \lambda_m(-A\cos\theta + \imath A\sin\theta) + (\lambda_i - \lambda_m)\sum_{k=1}^{N} \iint\limits_{D_k} \left(\frac{\partial T_k}{\partial x} - \imath\frac{\partial T_k}{\partial y}\right) dxdy.$$

Using (18), we have

$$\lambda_e^x(\theta) - \imath\lambda_e^y(\theta) = -A\lambda_m e^{-\imath\theta} + 2\lambda_m\rho \sum_{k=1}^{N} \iint\limits_{D_k} \psi_k(z)\, dxdy.$$

Due to the mean value theorem for harmonic functions, we finally obtain (66).

5.5 Appendix 2

This section contains the description of the Eisenstein function E_1 of first order. Properties of the Eisenstein functions of higher orders are described in details in [27].

The theory of elliptic functions provides the following formula for a lattice sum introduced by Rayleigh

$$S_{2n} := \sum_{m_1,m_2}{}' \frac{1}{(m_1 + \imath m_2)^{2n}}.$$

The Eisenstein functions of order p are defines as

$$E_p(z) := \sum_{m_1,m_2} (z - m_1 - \imath m_2)^{-p}.$$

The function E_2 and the Weierstrass function $\wp$ are related by the identities ([9])

$$E_2(z) := \wp(z) + S_2,$$

where $S_2 = \pi$ for the square array.

The derivative of the Eisenstein function possesses the following property:

$$E_p'(z) = -p \cdot E_{p+1}(z).$$

Using this relation, we have $E_1'(z) = -E_2(z)$. Thus, integration on $[0, z]$ gives

$$E_1(z) = \zeta(z) - \pi z,$$

where ζ is the Weierstrass zeta function, and $\zeta'(z) = -\wp(z)$.

Acknowledgements

The authors are grateful to Sergei Rogosin for fruitful discussions. ISOTOP's facilities, friendly environment and support during GM's secondment to the industrial partner in the PARM-2 project are greatly acknowledged.

References

[1] G. Allaire, *Shape Optimization by the Homogenization Method*, Berlin, Springer Verlag, 2002.

[2] I. V. Andrianov, V. I. Bolshakov, V. V. Danishevs'kyy, D. Weichert, *Higher order asymptotic homogenization and wave propagation in periodic composite materials*, Proc. R. Soc. London, 464 (2008), pp. 1181–1201.

[3] N. S. Bakhvalov, G. P. Panasenko, *Homogenization: Averaging Processes in Periodic Media*, Nauka, Moscow, 1984 (in Russian); English transl., Kluwer, Dordrecht/Boston/London, 1989.

[4] L. Berlyand, V. V. Mityushev, *Generalized Clausius–Mossotti formula for random composite with circular fibers*, J. Stat. Phys., 102 (2001), pp. 115–145.

[5] K. D. Cherednichenko, V. P. Smyshlyaev, *On full two-scale expansion of the solutions of nonlinear periodic rapidly oscillating problems and higher-order homogenised variational problems*, Arch. Ration. Mech. Anal, 174 (2004), pp. 385–442.

[6] K. D. Cherednichenko, V. P. Smyshlyaev, V. V. Zhikov, *Non-local homogenized limits for composite media with highly anisotropic periodic fibres* Proc. R. Soc. Edin., 136 (2006), pp. 87–114.

[7] A. V. Cherkaev, *Variational Methods for Structural Optimization*, New York, Springer Verlag, 2000.

[8] T. Fiedler, E. Pesetskaya, A. Oechsner, J. Grácio, *On the determination of the effective thermal conductivity of composite materials*, Proceedings of the 2. Workshop on Advanced Computational Engineering Mechanics, Erlangen, Germany, 30 June-2 July 2005, pp. 187–194.

[9] A. Hurwitz, *Lectures on General Function Theory and Elliptic Functions* (in German), Springer-Verlag, Berlin, 1964.

[10] V. V. Jikov, S. M. Kozlov, O. A. Oleinik, *Homogenization of Differential Operators and Integral Functionals*. Springer, Berlin, 1994.

[11] M. Kachanov, I. Tsukrov, B. Shafiro, *Effective moduli of solids with cavities of various shapes*, Appl. Mech. Rev., 47 (1994), pp. S151-S174.

[12] M. Kachanov, I. Sevostianov, *On quantitative characterization of microstructures and effective properties*, International Journal of Solids and Structures, 42 (2005), pp. 309-336.

[13] A. L. Kalamkarov, A. G. Kolpakov, *Analysis, Design and Optimization of Composite Structures*. Chichester, John Wiley & Sons, 1997.

[14] S. K. Kanaun, V. M Levin, *Self-Consistent Methods for Composites*, Springer, 2008.

[15] J. L. King, *A simple continuum model of a layered composite material*, J. of Strain Analysis for Engineering Design, 7 (1972), pp. 146–150.

[16] L. I. Manevitch, I. V. Andrianov, V. G. Oshmyan, *Mechanics of Periodically Heteregeneous Structures*, Foundations of Engineering Mechanics, Berlin, Springer. x + 264 p., 2002.

[17] K. Z. Markov, *Elementary Micromechanics of Heterogeneous Media. In Heterogeneous Media: Modelling and Simulation*, Ed. by K.Z. Markov and L. Preziosi, Birkhauser Boston, 1-162, 1999.

[18] G. W. Milton, *The Theory of Composites*, Cambridge Monographs on Applied and Computational Mathematics, 6, Cambridge University Press, Cambridge, 2002.

[19] G. W. Milton, *Mechanics of Composites*, Cambridge University Press, Cambridge, 2000.

[20] V. V. Mityushev, E. V. Pesetskaya, S. V. Rogosin, *Analytical methods for heat conduction in composites and porous media*, In: Thermal Properties of Cellular and Porous Materials, Amsterdam, WILEY-VCH, 2007, pp. 124–167.

[21] V. Mityushev, S. Rogosin, *Constructive Methods for Linear and Nonlinear Boundary Value Problems for Analytic Functions. Theory and Applications*, Monographs and Surveys in Pure and Applied Mathematics, 108, Chapman & Hall / CRC, Boca Raton, 1999.

[22] A. V. Movchan, N. V. Movchan, C. G. Poulton, *Asymptotic Models of Fields in Delute and Densely Packed Composites*, London, Imperial College Press, 2002.

[23] Yu. V. Obnosov, *Boundary Value Problems of the Theory of Heterogeneous Media: Multiphase Media, Separated by Second Order Curves*, Kazan, Kazan State University [in Russian], 2009.

[24] E. Pesetskaya, *Effective conductivity of composite materials with random positions of cylindrical inclusions: finite number inclusions in the cell*, Applicable Analysis, 84 (2005), No. 8, pp. 843–865.

[25] I. Sevostianov, M. Kachanov, *Connections between Elastic and Conductive Properties of Heterogeneous Materials*, Ed. by H. Aref and E. van der Giessen, Advances in Applied Mechanics, 42, Elsevier, pp. 69–252, 2008.

[26] W. M. Suen, S. P. Wong, K. Young, *The lattice model of heat conduction in a composite material*, J. Phys. D: Appl. Phys., 12 (1979), pp. 1325–1338.

[27] A. Weil, *Elliptic Functions According to Eisenstein and Kronecker*, Springer-Verlag, Berlin, 1976.

[28] T. I. Zohdi, P. Wriggers, *Introduction to Computational Micromechanics*, Springer, 2005.